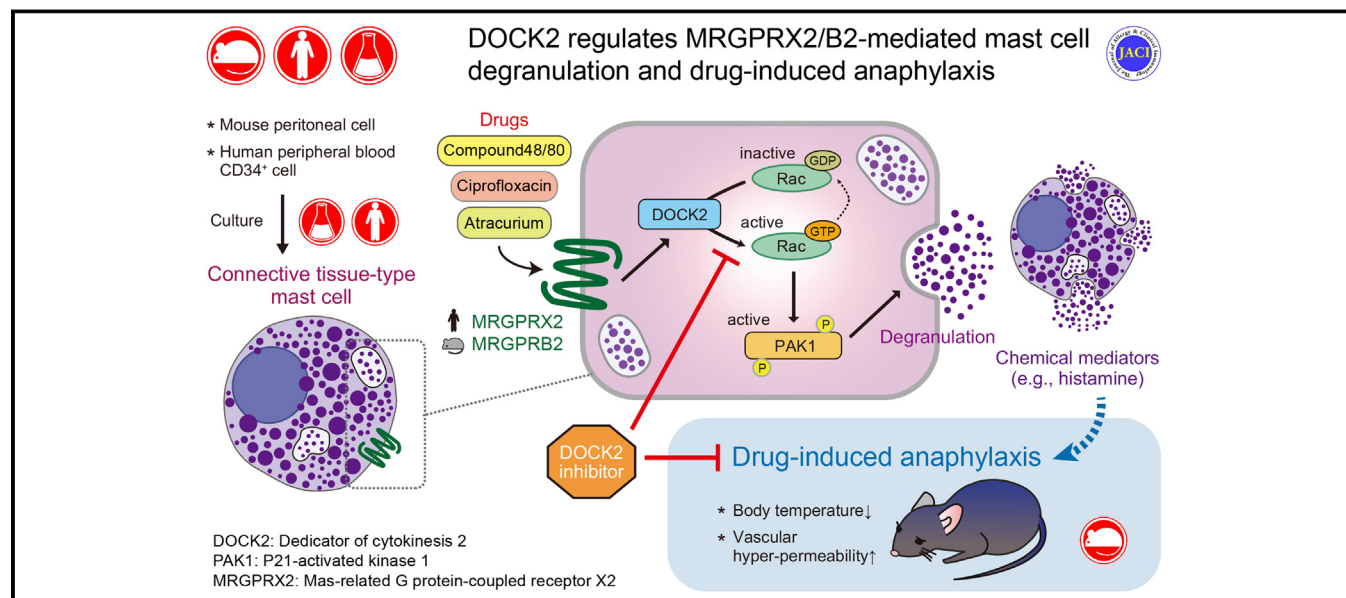


# DOCK2 regulates MRGPRX2/B2-mediated mast cell degranulation and drug-induced anaphylaxis



Kazufumi Kunimura, MD, PhD, Sayaka Akiyoshi, PhD, Takehito Uruno, PhD, Keisuke Matsubara, MS, Daiji Sakata, PhD, Kenji Morino, BSc, Kenichiro Hirotani, MD, and Yoshinori Fukui, MD, PhD *Fukuoka, Japan*

## GRAPHICAL ABSTRACT



**Background:** Drug-induced anaphylaxis is triggered by the direct stimulation of mast cells (MCs) via Mas-related G protein-coupled receptor X2 (MRGPRX2; mouse ortholog MRGPRB2). However, the precise mechanism that links MRGPRX2/B2 to MC degranulation is poorly understood. Dedicator of cytokinesis 2 (DOCK2) is a Rac activator predominantly expressed in hematopoietic cells. Although

DOCK2 regulates migration and activation of leukocytes, its role in MCs remains unknown.

**Objective:** We aimed to elucidate whether—and if so, how—DOCK2 is involved in MRGPRX2/B2-mediated MC degranulation and anaphylaxis.

**Methods:** Induction of drug-induced systemic and cutaneous anaphylaxis was compared between wild-type and DOCK2-deficient mice. In addition, genetic or pharmacologic inactivation of DOCK2 in human and murine MCs was used to reveal its role in MRGPRX2/B2-mediated signal transduction and degranulation.

**Results:** Induction of MC degranulation and anaphylaxis by compound 48/80 and ciprofloxacin was severely attenuated in the absence of DOCK2. Although calcium influx and phosphorylation of several signaling molecules were unaffected, MRGPRB2-mediated Rac activation and phosphorylation of p21-activated kinase 1 (PAK1) were impaired in DOCK2-deficient MCs. Similar results were obtained when mice or MCs were treated with small-molecule inhibitors that bind to the catalytic domain of DOCK2 and inhibit Rac activation.

**Conclusion:** DOCK2 regulates MRGPRX2/B2-mediated MC degranulation through Rac activation and PAK1 phosphorylation, thereby indicating that the DOCK2-Rac-PAK1 axis could be a target for preventing drug-induced anaphylaxis. (*J Allergy Clin Immunol* 2023;151:1585-94.)

**Key words:** Drug-induced anaphylaxis, mast cell, MRGPRX2, MRGPRB2, DOCK2, Rac, PAK1, phosphorylation, secretory granules

From the Department of Immunobiology and Neuroscience, Division of Immunogenetics, Medical Institute of Bioregulation, Kyushu University, Fukuoka.

Supported by the Japan Agency for Medical Research and Development (grants JP19ek0410064 and JP19gm1310005 to Y.F.), Japan Society for the Promotion of Science Grants-in-Aid for Scientific Research (grant JP21K15472 to K.K.), and the Qdai-jump Research Program (QR Program) of Kyushu University (grant 02243 to K.K.). Disclosure of potential conflict of interest: The authors declare that they have no relevant conflicts of interest.

Received for publication August 3, 2022; revised January 8, 2023; accepted for publication January 11, 2023.

Available online February 17, 2023.

Corresponding author: Kazufumi Kunimura, MD, PhD, Department of Immunobiology and Neuroscience, Division of Immunogenetics, Medical Institute of Bioregulation, Kyushu University, 3-1-1 Maidashi, Higashi-ku, Fukuoka 812-8582, Japan. E-mail: [kunimura@bioreg.kyushu-u.ac.jp](mailto:kunimura@bioreg.kyushu-u.ac.jp).

The CrossMark symbol notifies online readers when updates have been made to the article such as errata or minor corrections

0091-6749

© 2023 The Authors. Published by Elsevier Inc. on behalf of the American Academy of Allergy, Asthma & Immunology. This is an open access article under the CC BY license (<http://creativecommons.org/licenses/by/4.0/>).

<https://doi.org/10.1016/j.jaci.2023.01.029>

**Abbreviations used**

C48/80:	Compound 48/80
CS:	Cholesterol sulfate
DHR2:	DOCK homology region 2
DIA:	Drug-induced anaphylaxis
DMSO:	Dimethyl sulfoxide
DNP:	2,4-Dinitrophenol
DOCK:	Dedicator of cytokinesis
ERK1/2:	Extracellular signal-regulated kinase 1/2
GEF:	Guanine nucleotide exchange factor
GSK3 $\beta$ :	Glycogen synthase kinase 3 beta
HSA:	Human serum albumin
MAPK:	Mitogen-activated protein kinase
MC:	Mast cell
MRGPR:	Mas-related G protein-coupled receptor
PAK1:	P21-activated kinase 1
PBCMC:	Peripheral blood-derived cultured MC
PCMC:	Peritoneal cell-derived MC
WT:	Wild type

Drug-induced anaphylaxis (DIA) is a life-threatening allergic reaction that occurs immediately after drug intake.<sup>1</sup> Many small-molecule drugs are known to trigger pseudo-allergic reactions (also known as anaphylactoid reactions), which is a serious threat to public health.<sup>2,3</sup> DIA is characterized by more immediate and more systemic reactions than food- or venom-induced anaphylaxis and can arise without prior sensitization.<sup>1-3</sup> Notably, drugs are the most commonly reported cause of fatal anaphylaxis in many countries, including Japan and the United States.<sup>4,5</sup> Therefore, elucidation of the mechanism controlling DIA is important for preventive purposes.

Mast cells (MCs) play a key role in the induction of anaphylaxis. Once activated, MCs secrete preformed chemical mediators, including vasoactive amines (eg, histamine) and lysosomal enzymes such as  $\beta$ -hexosaminidase, which are stored in cytoplasmic secretory granules.<sup>6</sup> Although it is well established that degranulation of MCs is triggered by aggregation of the high-affinity IgE receptor Fc $\epsilon$ RI,<sup>6</sup> DIA is also caused by the direct stimulation of MCs via Mas-related G protein-coupled receptor X2 (MRGPRX2; mouse ortholog MRGPRB2).<sup>7-9</sup> McNeil et al<sup>7</sup> reported that the treatment with compound 48/80 (C48/80) or ciprofloxacin rapidly induced Ca<sup>2+</sup> reflux in murine peritoneal MCs and *Mrgprb2*-transfected HEK293 cells. Additionally, they showed that C48/80- or ciprofloxacin-induced Ca<sup>2+</sup> reflux and histamine release were abolished in peritoneal MCs derived from *Mrgprb2*-deficient mice,<sup>7</sup> demonstrating that these chemicals induce MC degranulation through MRGPRB2. Interestingly, recent evidence indicates that the size of granules and the kinetics of secretion are completely different between Fc $\epsilon$ RI-mediated and MRGPRX2/B2-mediated degranulation.<sup>10,11</sup> Therefore, it is likely that a different signaling cascade operates downstream of Fc $\epsilon$ RI and MRGPRX2/B2 during MC degranulation. However, the signaling cascade that links MRGPRX2/B2 to MC degranulation is poorly understood.

Dedicator of cytokinesis (DOCK) proteins comprise a family of evolutionarily conserved guanine nucleotide exchange factors (GEFs) for the Rho family of GTPases.<sup>12,13</sup> This family consists of 11 members, including DOCK2 and DOCK5.<sup>12,13</sup> Although both DOCK2 and DOCK5 act as the Rac-specific GEFs, the

GEF activity of DOCK2 in cells is much higher than that of DOCK5.<sup>14</sup> Previously, we showed that Rac activation by DOCK2 is essential for membrane polarization and cytoskeletal dynamics in various immune cell types—B cells,<sup>15,16</sup> T cells,<sup>17,18</sup> natural killer cells,<sup>19</sup> plasmacytoid dendritic cells,<sup>20</sup> and neutrophils.<sup>14,21</sup> However, little is known about the role of DOCK proteins in drug-induced MC degranulation. We have previously demonstrated that DOCK5 regulates Fc $\epsilon$ RI-mediated MC degranulation, independently of its Rac GEF activity, by controlling microtubule dynamics through phosphorylation and inactivation of glycogen synthase kinase 3 beta (aka GSK3 $\beta$ ).<sup>22</sup> In this study, we demonstrated that DOCK2, but not DOCK5, is essential for MRGPRX2/B2-mediated MC degranulation and anaphylactic responses. On the basis of these findings, we propose that the DOCK2–Rac–p21-activated kinase 1 (PAK1) signaling cascade could be a preventive target for DIA.

**METHODS****Mice**

The generation of *Dock2*<sup>-/-</sup> and *Dock5*<sup>-/-</sup> mice has been described previously.<sup>22,23</sup> Male and female mice at 8 to 12 weeks of age were used. *Dock2*<sup>-/-</sup> and *Dock5*<sup>-/-</sup> mice were backcrossed onto mice with a C57BL/6J background for more than 10 generations before use, and age- and sex-matched littermate *Dock2*<sup>+/+</sup> or *Dock5*<sup>+/+</sup> mice were used as wild-type (WT) controls. Mice were randomly selected and assigned to experimental groups according to genotype. All mice were maintained under specific-pathogen-free conditions at the animal facility of Kyushu University. All animal experiments were conducted according to the relevant national and international guidelines described in guidelines of the Act on Welfare and Management of Animals (Ministry of Environment of Japan) and Regulation of Laboratory Animals (Kyushu University). The ethics committee at Kyushu University approved the animal experiments (approval A22-032-0).

**Systemic and cutaneous anaphylaxis assay**

For induction of DIA, mice were injected intravenously (tail vein) with 100  $\mu$ L of C48/80 (1.5 mg/kg, Sigma-Aldrich, St Louis, Mo) or 100  $\mu$ L of ciprofloxacin (60 mg/kg, Sigma-Aldrich). To assess IgE-induced systemic anaphylaxis, mice were sensitized by intravenously injecting 10  $\mu$ g anti-2,4-dinitrophenol (DNP) mouse IgE antibody (SPE-7; Sigma-Aldrich) 24 hours before intravenous administration of 100  $\mu$ g DNP–human serum albumin (HSA; Sigma-Aldrich). In both cases, rectal temperatures were measured every 5 minutes for 30 minutes with a digital thermometer (Physitemp Instruments, Clifton, NJ). After 30 minutes, mice were humanely killed by decapitation, and blood samples were obtained after a cardiac puncture to measure the plasma histamine concentration with a histamine enzyme immunoassay kit (Beckman Coulter, Indianapolis, Ind). To examine the effects of cholesterol sulfate (CS),<sup>24</sup> mice were intraperitoneally administered 50  $\mu$ L of sodium cholesteryl sulfate (5 mg; Sigma-Aldrich) or vehicle (dimethyl sulfoxide [DMSO]; Wako, Osaka, Japan) 30 minutes before intravenous administration of ciprofloxacin or DNP-HSA. For the evaluation of cutaneous anaphylaxis, C48/80 or vehicle (PBS) was administered to the sole of the mouse's paw. Details for cutaneous anaphylaxis assay can be found in the Methods section of this article's Online Repository available at [www.jacionline.org](http://www.jacionline.org).

**Murine and human primary MC cultures**

Murine peritoneal cell-derived MCs (PCMCs) and human peripheral blood-derived cultured MCs (PBCMCs) were generated as described with a few modifications.<sup>25,26</sup> Details of the isolation, culture, and treatment of murine and human primary MC cultures are available in the Methods section of this article's Online Repository. Human peripheral blood samples were obtained from healthy volunteers (5 male subjects [mean  $\pm$  SD age, 30.0  $\pm$  5.2 years; range, 23–35 years] and 5 female subjects [mean  $\pm$  SD

age,  $29.4 \pm 5.5$  years; range, 23-37 years]) in compliance with institutional review board protocols. All study subjects were Japanese people living in Japan and were of Asian ethnicity. The experiments were approved by the ethics committee of Kyushu University, and written informed consent was obtained from all the volunteers before their participation according to the Helsinki Declaration.

### Flow cytometry and quantitative real-time PCR

Flow cytometric analysis was performed by a BD FACSVerser device equipped with BD FACSuite software (BD Biosciences, San Jose, Calif). Details for both flow cytometry and real-time quantitative PCR can be found in the Methods section of this article's Online Repository.

### MC degranulation assay

Murine PCMCs or human PBCMCs were seeded onto 96-well plates at a density of  $1 \times 10^5$  cells per well. Cells were treated with the vehicle (0.1% DMSO), sodium cholesteryl sulfate (Sigma-Aldrich), NVS-PAK1-1 (Abcam, Cambridge, United Kingdom), or CPYPP<sup>27</sup> for 30 minutes before stimulation. The synthesis and purification of CPYPP were performed by Kounosuke Oisaki (National Institute of Advanced Industrial Science and Technology, Tokyo Japan). Cells were stimulated for 30 minutes at 37°C with 10  $\mu\text{g}/\text{mL}$  C48/80, 400  $\mu\text{g}/\text{mL}$  ciprofloxacin, or 200  $\mu\text{g}/\text{mL}$  atracurium besylate (Santa Cruz Biotechnology, Santa Cruz, Calif) in Tyrode buffer (Sigma-Aldrich) in a final volume of 200  $\mu\text{L}$ . To assess IgE-induced degranulation levels, cells were sensitized with 1  $\mu\text{g}/\text{mL}$  anti-DNP mouse IgE antibody (SPE-7; Sigma-Aldrich) for 3 hours at 37°C and stimulated with 250 ng/mL DNP-HSA (Sigma-Aldrich) for 1 hour at 37°C. Details for  $\beta$ -hexosaminidase release assay are available in the Methods section of this article's Online Repository.

### Immunoblotting

To study Rac activation and the phosphorylation of signaling molecules, the cell extracts were prepared and immunoblotted as described in the Methods section of this article's Online Repository.

### Confocal microscopic analysis and histologic examination

PCMCs were stained for 20 minutes at 37°C with LysoTracker-Red (Thermo Fisher Scientific, Waltham, Mass) for visualization of secretory lysosomes. After stimulation with C48/80 (10  $\mu\text{g}/\text{mL}$ ), the cells were fixed with 4% paraformaldehyde (Wako) for 30 minutes. All images were obtained with a laser scanning confocal microscope (FV3000; Olympus, Tokyo, Japan). The method for toluidine blue staining can be found in the Methods section of this article's Online Repository.

### Calcium flux assay

PCMCs ( $1 \times 10^5$  cells) were treated with 3  $\mu\text{mol}$  Fura 2-AM (Dojindo Laboratories, Kumamoto, Japan) and 0.04% Pluronic F-127 (Biotium, Fremont, Calif) for 30 minutes at 37°C. Cells were resuspended in Tyrode buffer and stimulated with C48/80 (10  $\mu\text{g}/\text{mL}$ ). Fluorescence intensities were monitored at excitation wavelengths of 340 and 380 nm and at an emission wavelength of 510 nm with an EnVision multimode microplate reader (PerkinElmer, Waltham, Mass).

### Statistical analysis

Statistical analyses were performed by Prism 8 software (GraphPad Software, La Jolla, Calif). The data were initially tested by Kolmogorov-Smirnov test for normal distribution. Parametric data were analyzed by 2-tailed unpaired Student *t* test for comparison between 2 groups. Nonparametric data were analyzed by 2-tailed Mann-Whitney test for comparison between 2 groups. Statistical differences between more than 2 experimental

groups were evaluated by ANOVA with Dunnett or Bonferroni multiple comparison test. Data are expressed as means  $\pm$  SDs, and  $P < .05$  was considered significant.

## RESULTS

### DOCK2 is essential for induction of DIA *in vivo*

To examine whether DOCK2 and DOCK5 are involved in DIA, we treated WT, *Dock2*<sup>-/-</sup>, and *Dock5*<sup>-/-</sup> mice with the cationic polymer C48/80, which is also known to signal through MRGPRB2.<sup>7</sup> In response to C48/80, the rectal temperature of the WT and *Dock5*<sup>-/-</sup> mice dropped rapidly within 15 minutes (Fig 1, A). However, the rectal temperature was only modestly affected in the case of *Dock2*<sup>-/-</sup> mice (Fig 1, A), although the number of peritoneal and cutaneous MCs was comparable between WT and *Dock2*<sup>-/-</sup> mice (Fig E1, A and B). Consistently, *Dock2*<sup>-/-</sup> mice exhibited a marked reduction in plasma histamine concentration at 30 minutes after C48/80 injection compared to the WT and *Dock5*<sup>-/-</sup> mice (Fig 1, B, and see Fig E2 in the Online Repository available at [www.jacionline.org](http://www.jacionline.org)). Similar results were obtained when WT, *Dock2*<sup>-/-</sup>, and *Dock5*<sup>-/-</sup> mice were treated with a high dose of ciprofloxacin (fluoroquinolone antibiotic; see Fig E3 in the Online Repository). Thus, unexpectedly, DOCK2, but not DOCK5, is required for the induction of C48/80- and ciprofloxacin-induced systemic anaphylaxis.

To further examine the *in vivo* role of DOCK2 in DIA, we compared C48/80-induced cutaneous inflammation between WT and *Dock2*<sup>-/-</sup> mice after an intravenous injection with Evans blue dye. Representative images of the hind paws showed that cutaneous inflammation was weakened in *Dock2*<sup>-/-</sup> mice at 15 minutes after injection compared to WT mice (Fig 1, C). Indeed, we found that dye extravasation, which indicates vascular leakage, and paw swelling in response to C48/80 stimulation were reduced in *Dock2*<sup>-/-</sup> mice (Fig 1, D and E). Together, these results demonstrate that DOCK2 plays a key role in systemic and cutaneous anaphylaxis *in vivo*.

### DOCK2 controls MRGPRB2-mediated degranulation *in vitro*

Although bone marrow-derived MCs are primary cells used to examine Fc $\epsilon$ RI-mediated signals, they do not express MRGPRB2.<sup>28</sup> Therefore, to understand the role of DOCK2 and DOCK5 in MRGPRB2-mediated MC degranulation, we prepared connective tissue-type MCs via the isolation of peritoneal MCs and the culture with recombinant stem cell factor for 2 weeks (hereafter referred to as PCMCs). Untreated WT and *Dock2*<sup>-/-</sup> PCMCs have similar morphology (see Fig E4, A and B, in the Online Repository available at [www.jacionline.org](http://www.jacionline.org)), and the surface expression levels of the MC markers c-Kit and Fc $\epsilon$ RI were comparable between WT and *Dock2*<sup>-/-</sup> PCMCs (Fig 2, A). Similarly, quantitative real-time PCR analysis demonstrated that gene expression of *Mrgprb2*, *Fcer1a*, and *Kit* was unchanged between WT and *Dock2*<sup>-/-</sup> PCMCs (Fig 2, B). Because various drugs, including antibiotics and muscle relaxants, transmit the signals through MRGPRB2,<sup>29</sup> we analyzed drug-induced degranulation by stimulating PCMCs with C48/80, ciprofloxacin, and atracurium (a nonsteroidal neuromuscular blocking drug). Although WT and *Dock5*<sup>-/-</sup> PCMCs released considerable amounts of  $\beta$ -hexosaminidase (see Fig E5 in the Online Repository), a

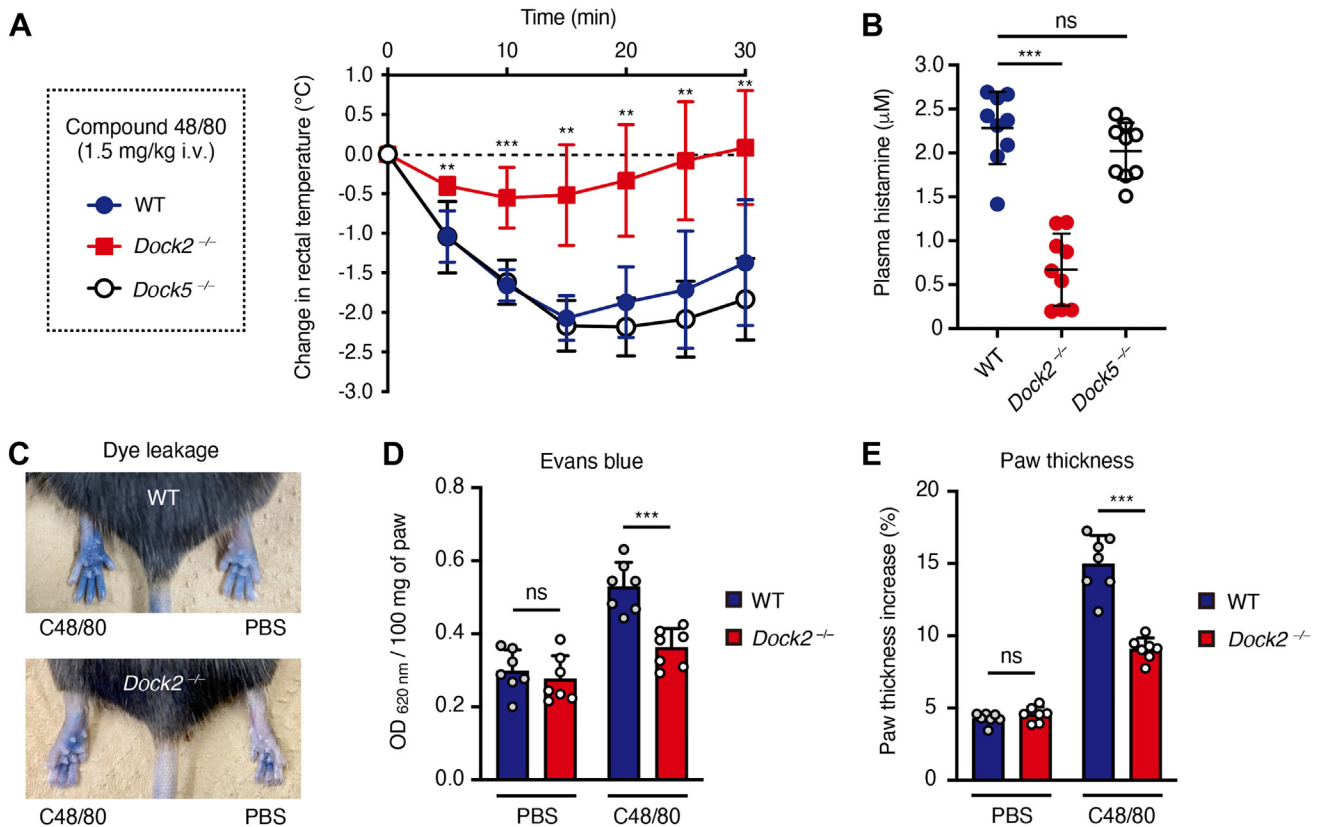


**FIG 1.** DOCK2 deficiency renders mice resistant to C48/80-induced systemic and cutaneous anaphylaxis. **A**, Change in rectal temperature in WT, *Dock2*<sup>-/-</sup>, and *Dock5*<sup>-/-</sup> mice challenged with C48/80 (n = 7; 2-way repeated-measures ANOVA with Dunnett multiple comparison test compared to WT). Mice were injected intravenously (tail vein) with 100  $\mu$ L C48/80 (1.5 mg/kg). **B**, Plasma histamine concentrations in WT, *Dock2*<sup>-/-</sup>, and *Dock5*<sup>-/-</sup> mice at 30 minutes after challenge with C48/80 (n = 9; 1-way ANOVA with Dunnett multiple comparison test). **C**, Representative images for dye leakage (n = 7 mice for each group) at 15 minutes after intraplantar injection of C48/80 (left) or PBS (right). **D** and **E**, Quantification of Evans blue leakage into paw (**D**) and increased paw thickness (**E**) after 15 minutes (n = 7; 2-tailed unpaired Student *t* test). Data were obtained from 3 independent experiments and are shown as means  $\pm$  SDs. \*\**P* < .01; \*\*\**P* < .001. NS, Not significant; *OD*<sub>620 nm</sub>, optical density at 620 nm.

protein stored in preformed MC granules, its release was severely impaired in the case of *Dock2*<sup>-/-</sup> PCMCs for all stimulants tested (Fig 2, C). This was further confirmed by staining WT and *Dock2*<sup>-/-</sup> PCMCs with LysoTracker. The LysoTracker-positive secretory granules were comparably detected in WT and *Dock2*<sup>-/-</sup> PCMCs before stimulation with C48/80 (Fig 2, D). However, although secretory granules rapidly disappeared in WT PCMCs, the granules were retained in the cytoplasm for longer periods in the absence of DOCK2 (Fig 2, D). Consistently, the degranulated granules around the cell membrane were observed in WT PCMCs, but not in *Dock2*<sup>-/-</sup> PCMCs under C48/80 stimulation (Fig E4, C). These results indicate that DOCK2 controls MRGPRB2-mediated MC degranulation.

### DOCK2 regulates MRGPRB2-mediated MC degranulation through Rac activation

To explore the mechanism by which DOCK2 regulates MRGPRB2-mediated MC degranulation, we first compared the phosphorylation and activation of the signaling molecules that are known to act downstream of MRGPRB2.<sup>30</sup> After C48/80 stimulation, Akt, GSK3 $\beta$ , p38 mitogen-activated protein kinase

(MAPK), and extracellular signal-regulated kinase 1/2 (ERK1/2; also called p44/42 MAPK) were comparably phosphorylated between WT and *Dock2*<sup>-/-</sup> PCMCs (Fig 3, A). In addition, MRGPRB2-mediated calcium influx was intact in *Dock2*<sup>-/-</sup> PCMCs (Fig 3, B). These results indicate that proximal signals downstream of MRGPRB2 operate normally even in the absence of DOCK2.

Although DOCK2 does not contain the Dbl homology domain typically found in GEFs, DOCK2 binds to Rac and mediates the GTP/GDP exchange reaction through DOCK homology region 2 (DHR2).<sup>12,13</sup> When WT PCMCs were stimulated with C48/80, GTP-bound activated Rac1 and Rac2 were readily detected at 10 and 30 s after stimulation (Fig 3, C and D). In contrast, C48/80-induced activation of Rac1/2 was significantly reduced in *Dock2*<sup>-/-</sup> PCMCs (Fig 3, C and D). This finding led us to examine whether DOCK2 regulates MRGPRB2-mediated MC degranulation through Rac activation. For this purpose, we used CS, a naturally occurring DOCK2 inhibitor that binds to the DHR2 domain of DOCK2 and suppresses its Rac GEF activity.<sup>24</sup> Both C48/80-induced Rac1/2 activation and  $\beta$ -hexosaminidase release were impaired when WT PCMCs were treated with 25–50  $\mu$ mol of CS (Fig 3, E–G). In contrast, CS treatment did not

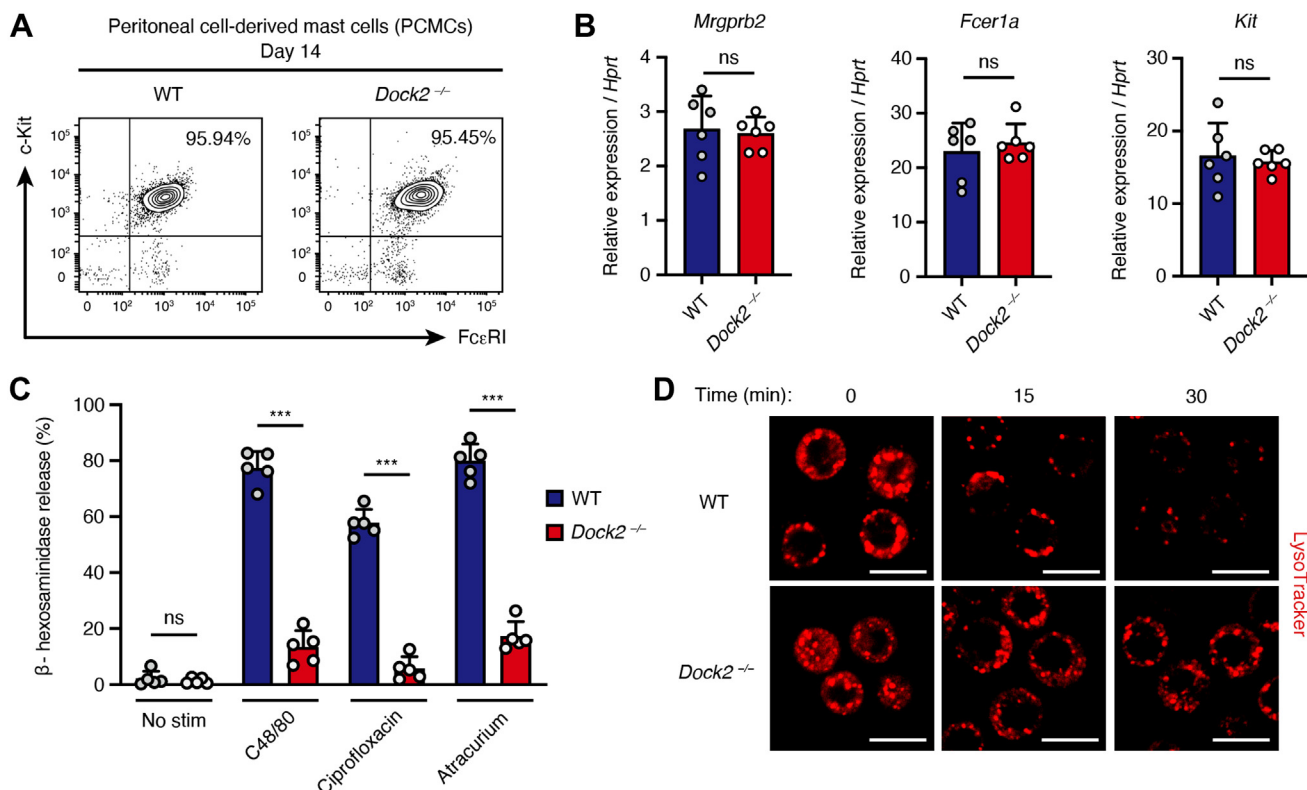


**FIG 2.** DOCK2 deficiency inhibits MRGPRB2-mediated MC degranulation. **A**, Flow cytometric analysis of PCMCs from WT and *Dock2*<sup>-/-</sup> mice. Percentage is shown of FcεRI<sup>+</sup>c-Kit<sup>+</sup> MCs in total cell culture. **B**, Messenger RNA expression of MC-specific genes in WT and *Dock2*<sup>-/-</sup> PCMCs was evaluated by real-time PCR (n = 6; 2-tailed unpaired Student *t* test). **C**, MRGPRB2-mediated degranulation of WT and *Dock2*<sup>-/-</sup> PCMCs were analyzed by β-hexosaminidase release assay after stimulation with C48/80, ciprofloxacin, and atracurium (n = 5; 2-tailed unpaired Student *t* test). **D**, Secretory granules in WT and *Dock2*<sup>-/-</sup> PCMCs were visualized by LysoTracker-Red at times indicated after C48/80 stimulation. Bar = 10 μm. Data were obtained from 5 (A and C), 3 (B), and 4 (D) independent experiments. Data are shown as means ± SDs. \*\*\**P* < .001. NS, Not significant.

visibly affect C48/80-induced Rac activation in *Dock2*<sup>-/-</sup> PCMCs (see Fig E6, A, in the Online Repository available at [www.jacionline.org](http://www.jacionline.org)). Furthermore, β-hexosaminidase release was also inhibited when WT PCMCs were treated with 50 μmol of CPYPP, a small-molecule inhibitor of DOCK2 that binds to the DHR2 domain (Fig E6, B).<sup>27</sup> Importantly, the concentration of CS and CPYPP used in these assays did not affect the viability of WT PCMCs at all (Fig E6, C). Thus, DOCK2 regulates MRGPRB2-mediated MC degranulation through Rac activation.

### Blockade of the DOCK2-Rac axis inhibits DIA *in vivo*

To investigate the effect of the DOCK2 inhibitor on DIA *in vivo*, WT mice were challenged with ciprofloxacin after intraperitoneal administration of CS or vehicle (Fig 4, A). When WT mice were treated with vehicle alone, they exhibited a progressive decrease in rectal temperature to 1.67 °C below the basal level at 20 minutes (Fig 4, B). In contrast, the rectal temperature was only modestly affected in the case of CS-treated mice (Fig 4, B). Consistent with this, the plasma concentration of histamine was significantly lower in CS-treated mice compared to vehicle-treated mice (Fig 4, C). These results indicate that pharmacologic blockade of the DOCK2-Rac axis can inhibit

MRGPRB2-mediated MC degranulation and anaphylactic responses. On the other hand, neither the genetic deletion of *Dock2* nor CS administration affected IgE-mediated MC degranulation and systemic anaphylaxis (see Fig E7 in the Online Repository available at [www.jacionline.org](http://www.jacionline.org)), indicating that the DOCK2-Rac axis is selectively involved in the MRGPRB2-mediated degranulation pathway.

### DOCK2-Rac signaling phosphorylates PAK1 acting downstream of MRGPRB2

Among the various effector molecules, PAK1 is a serine/threonine-specific kinase that is activated by Rac.<sup>31,32</sup> Although PAK1 was phosphorylated at Ser144 and Thr423 upon stimulation of WT PCMCs with C48/80, such a phosphorylation was significantly impaired in *Dock2*<sup>-/-</sup> PCMCs (Fig 5, A and B). Therefore, we hypothesized that reduction in PAK1 phosphorylation at Ser144 and Thr423 may lead to the impaired drug-induced degranulation in *Dock2*<sup>-/-</sup> PCMCs. To investigate this hypothesis, we analyzed C48/80-induced β-hexosaminidase release with or without treatment with NVS-PAK1-1,<sup>33</sup> a selective allosteric inhibitor of PAK1 kinase. We observed that C48/80-induced PAK1 phosphorylation at Ser144 and Thr423 at 2 minutes after

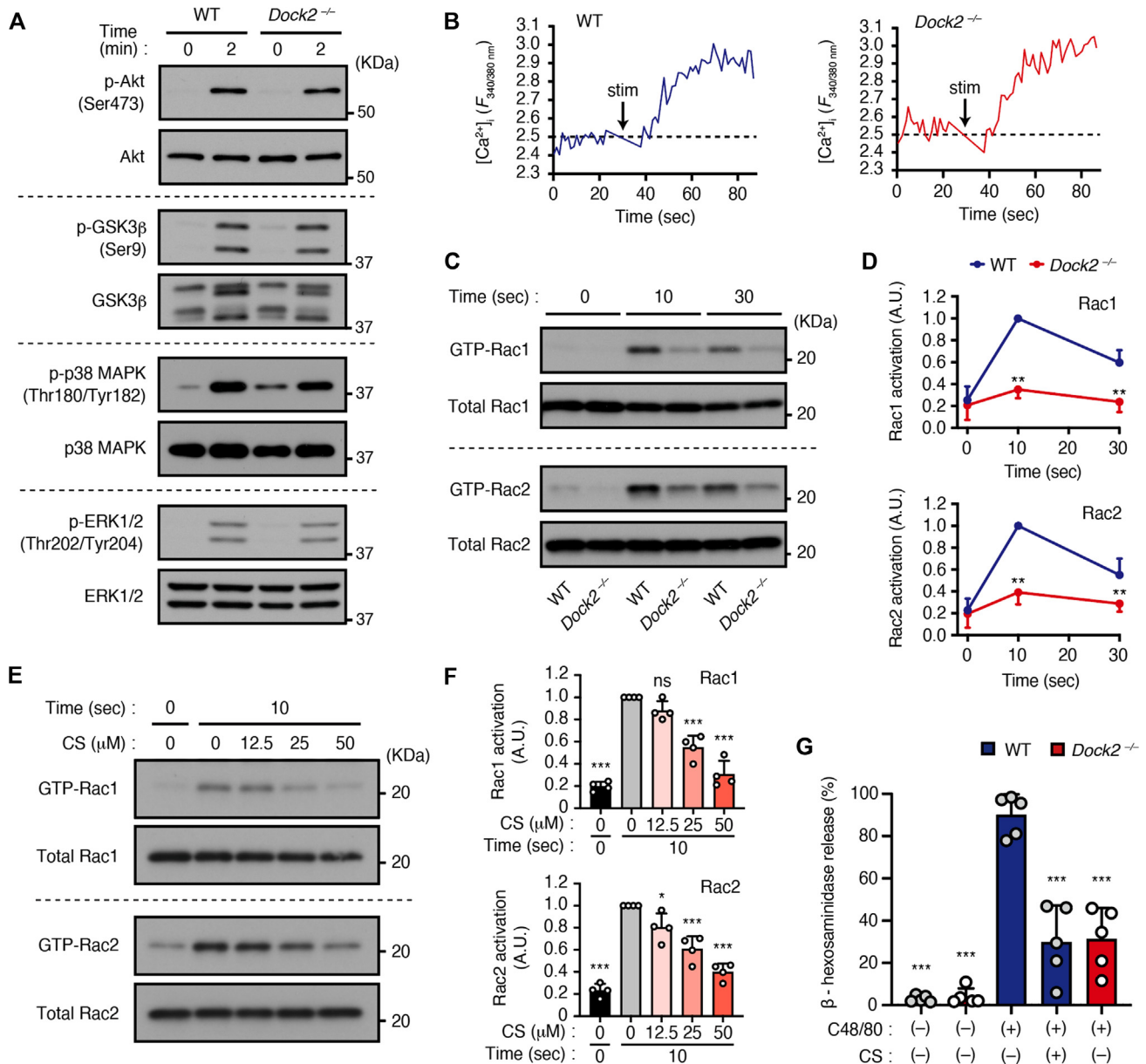


**FIG 3.** DOCK2 regulates C48/80-induced MC degranulation through Rac activation. **A**, Representative immunoblots showing phosphorylation of Akt, GSK3β, p38 MAPK, and ERK1/2 in WT and *Dock2*<sup>-/-</sup> PCMCs followed by stimulation with C48/80 for 0 or 2 minutes. **B**, Intracellular calcium ion flux in Fura 2-AM-loaded PCMCs after C48/80 stimulation. Data are indicated as Fura 2-AM ratio at 340:380 nm. **C** and **D**, Representative immunoblots showing C48/80-induced Rac activation in WT and *Dock2*<sup>-/-</sup> PCMCs (**C**). Data (n = 5, 2-tailed Mann-Whitney test) are presented as ratio of GTP-bound Rac1/2 to total Rac1/2 after setting 10-second value of WT sample to an arbitrary unit (AU) of 1 (**D**). **E** and **F**, Representative immunoblots showing effect of CS on C48/80-induced Rac activation in WT PCMCs (**E**). Data (n = 4, 1-way ANOVA with Dunnett multiple comparison test) are presented as ratio of GTP-bound Rac1/2 to total Rac1/2 after setting 10-second value of control sample to an arbitrary unit of 1 (**F**). **G**, C48/80-induced degranulation of PCMCs after treatment with 50 μmol CS was analyzed by β-hexosaminidase release assay (n = 5; 1-way ANOVA with Dunnett multiple comparison test). Data were obtained from 4 (**A** and **F**) and 5 (**B**, **D**, and **G**) independent experiments. Data are shown as means ± SDs. \**P* < .05; \*\**P* < .01; \*\*\**P* < .001. NS, Not significant.

stimulation was suppressed by treatment with NVS-PAK1-1 (Fig 5, C and D). Importantly, NVS-PAK1-1 inhibited C48/80-induced β-hexosaminidase release in a dose-dependent manner (Fig 5, E). These results indicate that the DOCK2-Rac-PAK1 axis regulates MRGPRB2-mediated MC degranulation.

### DOCK2-Rac-PAK1 signaling pathway is also required for MRGPRX2-mediated degranulation in human MCs

Finally, we examined whether DOCK2-Rac signaling is also critical for MRGPRX2-mediated degranulation of human MCs.

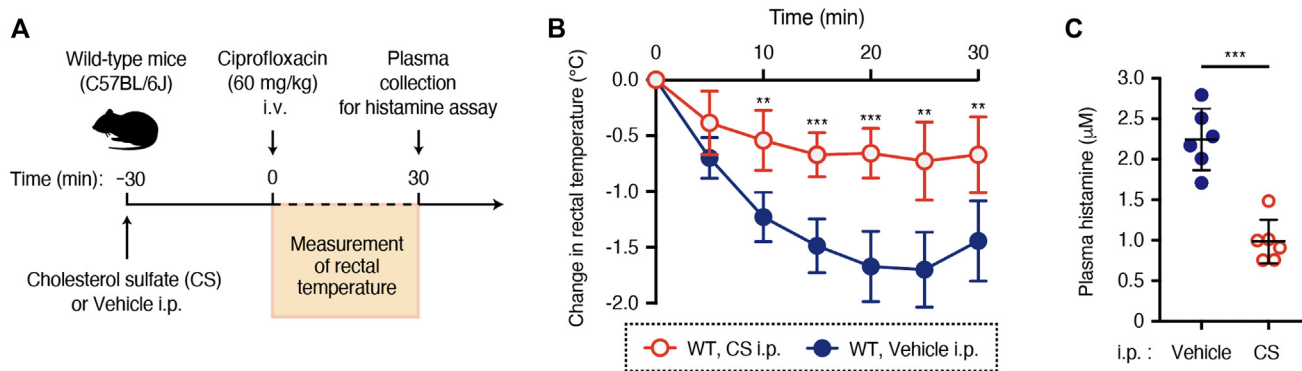


**FIG 4.** Treatment with a DOCK2 inhibitor inhibits DIA *in vivo*. **A**, Experimental protocol for ciprofloxacin-induced systemic anaphylaxis model after intraperitoneal administration of CS or vehicle. **B**, Change in rectal temperature in WT mice challenged with ciprofloxacin ( $n = 7$ , 2-way repeated-measures ANOVA with Bonferroni multiple comparison test). **C**, Plasma histamine concentrations in WT mice challenged with ciprofloxacin ( $n = 6$ , 2-tailed unpaired Student *t* test). Data were obtained from 3 (**B** and **C**) independent experiments. Data are shown as means  $\pm$  SDs. \*\* $P < .01$ ; \*\*\* $P < .001$ .

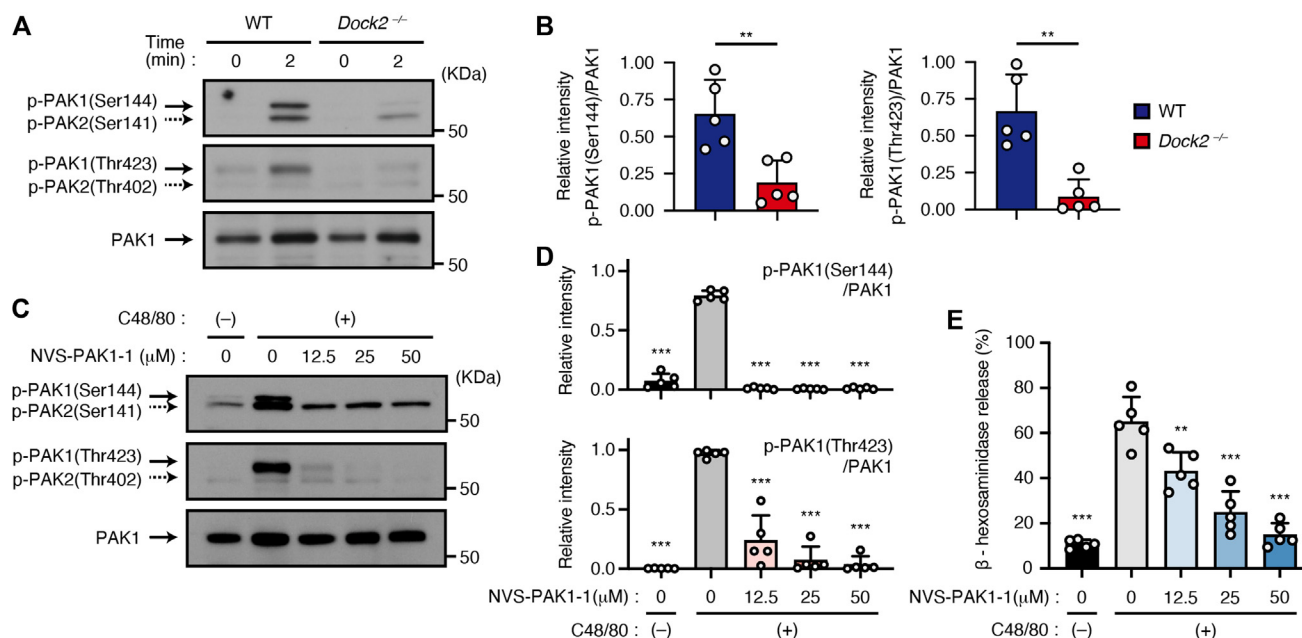


**FIG 5.** DOCK2 regulates phosphorylation of PAK1 upon stimulation with C48/80. **A**, Representative immunoblots showing phosphorylation of PAK1 in WT and *Dock2*<sup>-/-</sup> PCMCs, followed by stimulation with C48/80 for 0 or 2 minutes. **B**, Results of 5 individual blots for PAK1 phosphorylation quantified by densitometry and shown as relative intensity of p-PAK1 (Ser144 and Thr423) to total PAK1 protein ( $n = 5$ ; 2-tailed unpaired Student *t* test). **C**, Representative immunoblots showing phosphorylation of PAK1 in WT PCMCs after treatment with NVS-PAK1-1, an allosteric PAK1 inhibitor. **D**, Results of 5 individual blots shown as relative intensity of p-PAK1 to total PAK1 protein ( $n = 5$ ; 1-way ANOVA with Dunnett multiple comparison test). **E**, C48/80-induced degranulation of WT PCMCs after treatment with NVS-PAK1-1 was analyzed by  $\beta$ -hexosaminidase release assay ( $n = 5$ ; 1-way ANOVA with Dunnett multiple comparison test). Data were obtained from 5 independent experiments and are shown as means  $\pm$  SDs. \*\* $P < .01$ ; \*\*\* $P < .001$ .

Because human DOCK2 deficiency is a rare disorder,<sup>34</sup> we generated human PBCMCs from healthy donors and investigated whether CS could block MRGPRX2-mediated MC degranulation. Before assays, human PBCMCs were verified to express c-Kit, Fc $\epsilon$ RI, and MRGPRX2 by flow cytometry (Fig 6, A). When male and female PBCMCs were pretreated with CS, ciprofloxacin-induced  $\beta$ -hexosaminidase release was suppressed in a manner dependent on the CS concentration (Fig 6, B). Moreover, NVS-PAK1-1 inhibited ciprofloxacin-induced

$\beta$ -hexosaminidase release (Fig 6, C). These data indicated that the DOCK2-Rac-PAK1 signaling pathway is also required for MRGPRX2-mediated MC degranulation in humans, irrespective of gender.

## DISCUSSION

DIA is a life-threatening allergic reaction that occurs quickly after drug intake. Although MRGPRX2 (mouse ortholog

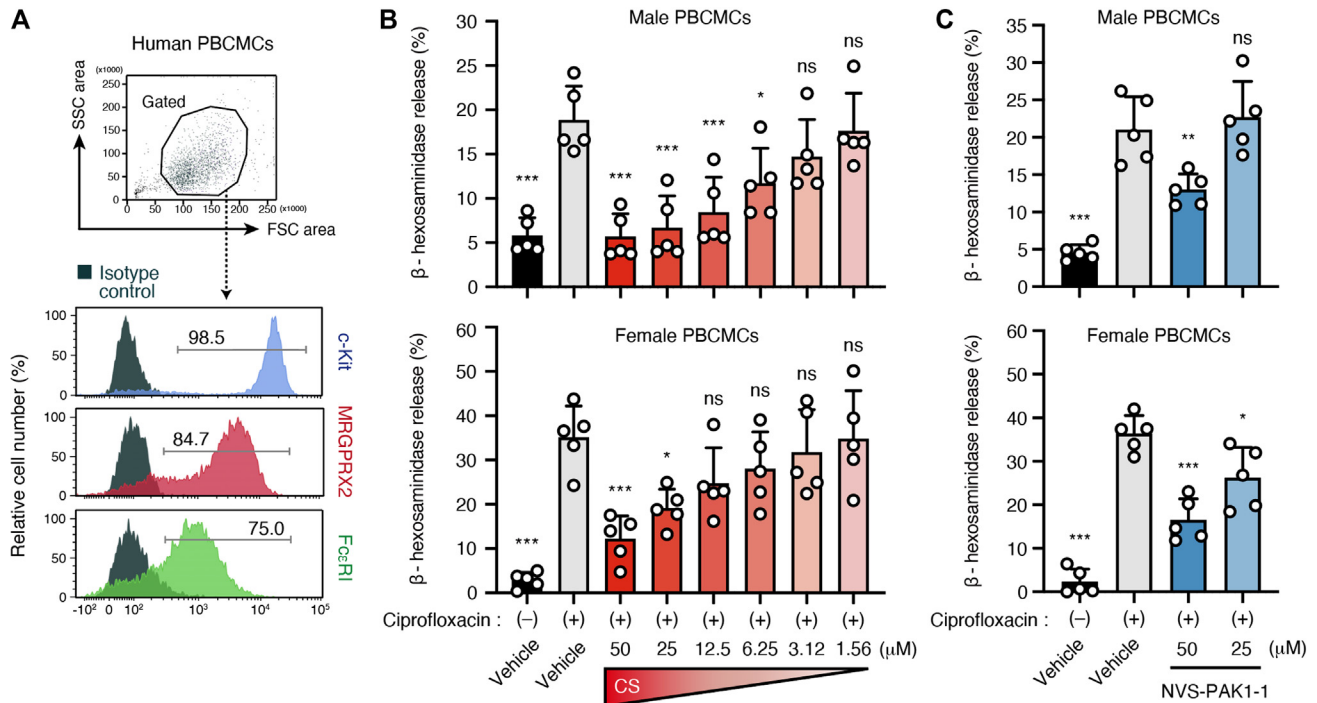


**FIG 6.** DOCK2 inhibitor blocks ciprofloxacin-induced degranulation in human MCs. **A**, Surface expression levels of c-Kit, FcεRI, or MRGPRX2 in human PBCMCs from a healthy donor. Isotype controls are shown as navy blue histograms. Data are representative of 5 independent experiments. **B** and **C**, MRGPRX2-mediated degranulation of human PBCMCs derived from male and female subjects was analyzed by β-hexosaminidase release assay after stimulation with 400 μg/mL ciprofloxacin ( $n = 5$ ; 1-way ANOVA with Dunnett multiple comparison test). Cells were treated with vehicle (0.1% DMSO), CS (**B**), or NVS-PAK1-1 (**C**) for 30 minutes before stimulation. Data were obtained from 5 (**B** and **C**) independent experiments. Data are shown as means  $\pm$  SDs. \* $P < .05$ ; \*\* $P < .01$ ; \*\*\* $P < .001$ . NS, Not significant.

MRGPRB2), the recently described G protein-coupled receptor, plays a key role in induction of DIA,<sup>7-9</sup> the signaling cascade that links MRGPRX2/B2 to MC degranulation is largely unknown. Here we provide evidence that DOCK2, but not DOCK5, is essential for MRGPRX2/B2-mediated MC degranulation *in vitro* and anaphylactic responses *in vivo*. We found that MRGPRB2-mediated activation of Rac1 and Rac2 was severely impaired in *Dock2*<sup>-/-</sup> PCMCs. In addition, MRGPRX2/B2-mediated MC degranulation was abolished when murine and human PCMCs were treated with the DOCK2 inhibitors CS and CPYPP,<sup>24,27</sup> which bind to the DHR2 domain and block its Rac GEF activity. Collectively, these results indicate that DOCK2 regulates MRGPRX2/B2-mediated degranulation through Rac activation.

Recent evidence indicates that unlike FcεRI-mediated degranulation, MRGPRX2/B2-mediated degranulation occurs rapidly and is characterized by direct release of small, spherical granules from all over the MC surface.<sup>10,11</sup> The precise mechanism of how DOCK2-mediated Rac activation regulates MRGPRX2/B2-mediated degranulation remains to be determined. However, we have identified the serine/threonine kinase PAK1 as a critical signaling molecule that controls MRGPRX2/B2-mediated degranulation. PAK1 has 2 autophosphorylation sites, Ser144 (in the N-terminal autoinhibitory domain; residues 70-149) and Thr423 (in the C-terminal catalytic kinase domain; residues 272-523), the phosphorylation of which leads to releasing autoinhibition and enhancing kinase activity, respectively.<sup>35-37</sup> In this study, on the one hand, we have shown that C48/80-induced PAK1 phosphorylation at Ser144 and Thr423 was severely

impaired in *Dock2*<sup>-/-</sup> PCMCs, indicating that DOCK2-mediated Rac activation is required for MRGPRX2/B2-mediated PAK1 phosphorylation. On the other hand, the MRGPRX2/B2-mediated degranulation of murine PCMCs and human PBCMCs was attenuated by treatment with NVS-PAK1-1,<sup>33</sup> which potently inhibits PAK1 autophosphorylation. Interestingly, it has been reported that activated PAK1 regulates ezrin/radixin/moesin proteins that uncouple the plasma membrane from actin before exocytosis.<sup>38</sup> Therefore, DOCK2-mediated Rac activation may facilitate membrane opening and exocytosis through PAK1 phosphorylation during MRGPRX2/B2-mediated degranulation.

A growing number of recent articles have suggested that in addition to DIA, MRGPRX2 expressed on MCs plays important roles in the pathogenesis of various allergic diseases.<sup>39-43</sup> For example, the number and percentage of MRGPRX2-expressing MCs in the skin are much higher in patients with severe chronic urticaria than in nonatopic control subjects.<sup>44</sup> In addition, messenger RNA expression of MRGPRX2 is upregulated in skin biopsy samples from patients with maculopapular cutaneous mastocytosis compared to healthy controls.<sup>45</sup> Furthermore, it has been reported that the preservative thimerosal, which is known to cause contact dermatitis, induces MC degranulation via MRGPRX2.<sup>46</sup> Thus, there is a possibility that MRGPRX2-mediated MC activation is involved in the pathogenesis of these allergic diseases. Here we have demonstrated that DOCK2 regulates MRGPRX2/B2-mediated MC degranulation and anaphylactic responses through Rac activation and PAK1



phosphorylation. Therefore, the DOCK2-Rac-PAK1 axis may be a therapeutic target for controlling MRGPRX2-related allergic disorders including DIA.

We thank Ayumi Inayoshi, Arisa Aosaka, Nao Kanematsu, Satomi Hori, and Aya Nishino at Kyushu University for their technical assistance. We also thank Kounosuke Oisaki at the National Institute of Advanced Industrial Science and Technology for the synthesis of CPYPP. We appreciate the help of Ichita Hasegawa during the initial phase of this study. In addition, we thank the Medical Research Center Initiative for High Depth Omics, Kyushu University, for their support.

### Key messages

- DOCK2 deficiency renders mice resistant to drug-induced systemic and cutaneous anaphylaxis.
- DOCK2 acts downstream of MRGPRX2/B2 and regulates drug-induced MC degranulation through Rac activation and PAK1 phosphorylation.
- Small-molecule inhibitors of DOCK2 can block drug-induced MC degranulation *in vitro* and anaphylaxis *in vivo*.

### REFERENCES

1. Montañez MI, Mayorga C, Bogas G, Barrionuevo E, Fernandez-Santamaria R, Martin-Serrano A, et al. Epidemiology, mechanisms, and diagnosis of drug-induced anaphylaxis. *Front Immunol* 2017;8:614.
2. Zhang B, Li Q, Shi C, Zhang X. Drug-induced pseudoallergy: a review of the causes and mechanisms. *Pharmacology* 2018;101:104-10.
3. Regateiro FS, Marques ML, Gomes ER. Drug-induced anaphylaxis: an update on epidemiology and risk factors. *Int Arch Allergy Immunol* 2020;181:481-7.
4. Medical Accident Investigation and Support Center; Japan Medical Safety Research Organization. Analysis of deaths related to anaphylaxis caused by injections. January 2018. Available at: [https://www.medsafe.or.jp/modules/en/index.php?content\\_id=15](https://www.medsafe.or.jp/modules/en/index.php?content_id=15).
5. Yu RJ, Krantz MS, Phillips EJ, Stone CA. Emerging causes of drug-induced anaphylaxis: a review of anaphylaxis-associated reports in the FDA Adverse Event Reporting System (FAERS). *J Allergy Clin Immunol Pract* 2020;9:819-29.
6. Ménasché G, Longé C, Bratti M, Blank U. Cytoskeletal transport, reorganization, and fusion regulation in mast cell–stimulus secretion coupling. *Front Cell Dev Biol* 2021;9:652077.
7. McNeil BD, Pundir P, Meeker S, Han L, Udem BJ, Kulka M, et al. Identification of a mast-cell–specific receptor crucial for pseudo-allergic drug reactions. *Nature* 2015;519:237-41.
8. Porebski G, Kwiecien K, Pawica M, Kwitniewski M. Mas-related G protein–coupled receptor-X2 (MRGPRX2) in drug hypersensitivity reactions. *Front Immunol* 2018;9:3027.
9. McNeil BD. MRGPRX2 and adverse drug reactions. *Front Immunol* 2021;12:676354.
10. Gaudenzio N, Sibilano R, Marichal T, Starkl P, Reber LL, Cenac N, et al. Different activation signals induce distinct mast cell degranulation strategies. *J Clin Invest* 2016;126:3981-98.
11. Karhausen J, Abraham SN. How mast cells make decisions. *J Clin Invest* 2016;126:3735-8.
12. Kunimura K, Uruno T, Fukui Y. DOCK family proteins: key players in immune surveillance mechanisms. *Int Immunol* 2020;32:5-15.
13. Laurin M, Côté JF. Insights into the biological functions of Dock family guanine nucleotide exchange factors. *Genes Dev* 2014;28:533-47.
14. Watanabe M, Terasawa M, Miyano K, Yanagihara T, Uruno T, Sanematsu F, et al. DOCK2 and DOCK5 act additively in neutrophils to regulate chemotaxis, superoxide production, and extracellular trap formation. *J Immunol* 2014;193:5660-7.
15. Ushijima M, Uruno T, Nishikimi A, Sanematsu F, Kamikaseda Y, Kunimura K, et al. The Rac activator DOCK2 mediates plasma cell differentiation and IgG antibody production. *Front Immunol* 2018;9:243.
16. Jing Y, Kang D, Liu L, Huang H, Chen A, Yang L, et al. Deducator of cytokinesis protein 2 couples with lymphoid enhancer–binding factor 1 to regulate expression of CD21 and B-cell differentiation. *J Allergy Clin Immunol* 2019;144:1377-90.e4.
17. Tanaka Y, Hamano S, Gotoh K, Murata Y, Kunisaki Y, Nishikimi A, et al. T helper type 2 differentiation and intracellular trafficking of the interleukin 4 receptor-alpha subunit controlled by the Rac activator Dock2. *Nat Immunol* 2007;8:1067-75.
18. Ackerknecht M, Gollmer K, Germann P, Ficht X, Abe J, Fukui Y, et al. Antigen availability and DOCK2-driven motility govern CD4<sup>+</sup> T cell interactions with dendritic cells *in vivo*. *J Immunol* 2017;199:520-30.
19. Sakai Y, Tanaka Y, Yanagihara T, Watanabe MS, Duan X, Terasawa M, et al. The Rac activator DOCK2 regulates natural killer cell–mediated cytotoxicity in mice through the lytic synapse formation. *Blood* 2013;122:386-93.
20. Gotoh K, Tanaka Y, Nishikimi A, Nakamura R, Yamada H, Maeda N, et al. Selective control of type I IFN induction by the Rac activator DOCK2 during TLR-mediated plasmacytoid dendritic cell activation. *J Exp Med* 2010;207:721-30.
21. Nishikimi A, Fukuhara H, Su W, Hongu T, Takasuga S, Mihara H, et al. Sequential regulation of DOCK2 dynamics by two phospholipids during neutrophil chemotaxis. *Science* 2009;324:384-7.
22. Ogawa K, Tanaka Y, Uruno T, Duan X, Harada Y, Sanematsu F, et al. DOCK5 functions as a key signaling adaptor that links FcεRI signals to microtubule dynamics during mast cell degranulation. *J Exp Med* 2014;211:1407-19.
23. Fukui Y, Hashimoto O, Sanui T, Oono T, Koga H, Abe M, et al. Haematopoietic cell–specific CDM family protein DOCK2 is essential for lymphocyte migration. *Nature* 2001;412:826-31.
24. Sakurai T, Uruno T, Sugiura Y, Tatsuguchi T, Yamamura K, Ushijima M, et al. Cholesterol sulfate is a DOCK2 inhibitor that mediates tissue-specific immune evasion in the eye. *Sci Signal* 2018;11:eaao4874.
25. Takamori A, Izawa K, Kaitani A, Ando T, Okamoto Y, Maehara A, et al. Identification of inhibitory mechanisms in pseudo-allergy involving Mrgrprb2/MRGPRX2-mediated mast cell activation. *J Allergy Clin Immunol* 2019;143:1231-5.e12.
26. Folkerts J, Gaudenzio N, Maurer M, Hendriks RW, Stadhouders R, Tam SY, et al. Rapid identification of human mast cell degranulation regulators using functional genomics coupled to high-resolution confocal microscopy. *Nat Protoc* 2020;15:1285-310.
27. Nishikimi A, Uruno T, Duan X, Cao Q, Okamura Y, Saitoh T, et al. Blockade of inflammatory responses by a small-molecule inhibitor of the Rac activator DOCK2. *Chem Biol* 2012;19:488-97.
28. Akula S, Paivandy A, Fu Z, Thorpe M, Pejler G, Hellman L. How relevant are bone marrow–derived mast cells (BMMCs) as models for tissue mast cells? A comparative transcriptome analysis of BMMCs and peritoneal mast cells. *Cells* 2020;9:2118.
29. McNeil BD. Minireview: Mas-related G protein–coupled receptor X2 activation by therapeutic drugs. *Neurosci Lett* 2021;751:135746.
30. Ogasawara H, Noguchi M. Therapeutic potential of MRGPRX2 inhibitors on mast cells. *Cells* 2021;10:2906.
31. Kichina JV, Goc A, Al-Husein B, Somanath PR, Kandel ES. PAK1 as a therapeutic target. *Expert Opin Ther Targets* 2010;14:703-25.
32. Chiang YA, Jin T. p21-Activated protein kinases and their emerging roles in glucose homeostasis. *Am J Physiol Endocrinol Metab* 2014;306:E707-22.
33. Karpov AS, Amiri P, Bellamacina C, Bellance MH, Breitenstein W, Daniel D, et al. Optimization of a dibenzodiazepine hit to a potent and selective allosteric PAK1 inhibitor. *ACS Med Chem Lett* 2015;6:776-81.
34. Dobbs K, Domínguez Conde C, Zhang SY, Parolini S, Audry M, Chou J, et al. Inherited DOCK2 deficiency in patients with early-onset invasive infections. *N Engl J Med* 2015;372:2409-22.
35. Lei M, Lu W, Meng W, Parrini MC, Eck MJ, Mayer BJ, et al. Structure of PAK1 in an autoinhibited conformation reveals a multistage activation switch. *Cell* 2000;102:387-97.
36. Radu M, Semenova G, Kosoff R, Chernoff J. PAK signalling during the development and progression of cancer. *Nat Rev Cancer* 2014;14:13-25.
37. Yao D, Li C, Rajoka MSR, He Z, Huang J, Wang J, et al. P21-activated kinase 1: emerging biological functions and potential therapeutic targets in cancer. *Theranostics* 2020;10:9741-66.
38. Staser K, Shew MA, Michels EG, Mwanthi MM, Yang FC, Clapp DW, et al. A Pak1-PP2A-ERM signaling axis mediates F-actin rearrangement and degranulation in mast cells. *Exp Hematol* 2013;41:56-66.
39. Roy S, Chompuud Na Ayudhya C, Thapaliya M, Deepak V, Ali H. Multifaceted MRGPRX2: new insight into the role of mast cells in health and disease. *J Allergy Clin Immunol* 2021;148:293-308.
40. Kühn H, Kolkhir P, Babina M, Düll M, Frischbutter S, Fok JS, et al. Mas-related G protein–coupled receptor X2 and its activators in dermatologic allergies. *J Allergy Clin Immunol* 2021;147:456-69.
41. Quan PL, Sabaté-Brescó M, Guo Y, Martín M, Gastaminza G. The multifaceted Mas-related G protein–coupled receptor member X2 in allergic diseases and beyond. *Int J Mol Sci* 2021;22:4421.

42. An J, Lee J, Won H, Kang Y, Song W, Kwon H, et al. Clinical significance of serum MRGPRX2 as a new biomarker in allergic asthma. *Allergy* 2020;75:959-62.
43. Wang Z, Babina M. MRGPRX2 signals its importance in cutaneous mast cell biology: does MRGPRX2 connect mast cells and atopic dermatitis? *Exp Dermatol* 2020;29:1104-11.
44. Fujisawa D, Kashiwakura J, Kita H, Kikukawa Y, Fujitani Y, Sasaki-Sakamoto T, et al. Expression of Mas-related gene X2 on mast cells is upregulated in the skin of patients with severe chronic urticaria. *J Allergy Clin Immunol* 2014;134:622-33.
45. Deepak V, Komarow HD, Alblaihees AA, Carter MC, Metcalfe DD, Ali H. Expression of MRGPRX2 in skin mast cells of patients with maculopapular cutaneous mastocytosis. *J Allergy Clin Immunol Pract* 2021;9:3841-3.e1.
46. Peng B, Che D, Hao Y, Zheng Y, Liu R, Qian Y, et al. Thimerosal induces skin pseudo-allergic reaction via Mas-related G-protein coupled receptor B2. *J Dermatol Sci* 2019;95:99-106.

## METHODS

### Cutaneous anaphylaxis assay

Mice were injected intravenously with 150  $\mu$ L of 0.4% Evans blue dye (Wako) in PBS. Five minutes later, 5  $\mu$ L of C48/80 (150 ng) was administered on the sole of the left paw, and an equal volume of PBS was administered to the right paw. Paw thickness was measured with a digital thickness gauge (Mitutoyo, Kanagawa, Japan) after injection. After 15 minutes, paw thickness was measured again, and the mice were humanely killed by decapitation. The paws were excised, dried at 55°C overnight, weighed separately, and incubated in acetone-saline (7:3, 500  $\mu$ L) for 24 hours at 37°C. The supernatant solution (150  $\mu$ L) after treatment with acetone-saline (7:3, 500  $\mu$ L) was measured with an absorbance spectrophotometer.

### Murine and human primary MC cultures

Murine PCMCs were generated as described previously with some modifications.<sup>E1</sup> Briefly, after intraperitoneal injection of cold PBS, peritoneal cells were obtained from mice and cultured in 4 mL Dulbecco modified Eagle medium (Wako) with 10% (vol/vol) heat-inactivated fetal bovine serum (Thermo Fisher Scientific), 50  $\mu$ mol 2-mercaptoethanol (Nacalai Tesque, Kyoto, Japan), 100 U/mL penicillin, 100  $\mu$ g/mL streptomycin, 2 mmol L-glutamine, 1 mmol sodium pyruvate, 1 $\times$  minimum essential medium nonessential amino acids (all from Thermo Fisher Scientific), and 25 ng/mL recombinant mouse stem cell factor (SCF; PeproTech, Rocky Hill, NJ). The medium was changed every 3 or 4 days during culture, and floating cells were collected on day 14 for assay. Cell purity was confirmed by analyzing c-Kit and Fc $\epsilon$ RI expression by flow cytometry.

Human PBCMCs were generated as described previously with some modifications.<sup>E2</sup> Briefly, CD34<sup>+</sup> peripheral blood cells were isolated from peripheral mononuclear cells using the Human CD34 Positive Selection Kit II (STEMCELL Technologies, Vancouver, British Columbia, Canada) and cultured in StemSpan Serum-Free Expansion Medium II (SFEM II; STEMCELL Technologies) containing 50 ng/mL recombinant human (rh) SCF, 50 ng/mL rhIL-6, 10 ng/mL rhIL-3 (all from PeproTech), and 10  $\mu$ g/mL ciprofloxacin (Sigma-Aldrich) for 4 weeks. According to the protocol reported by Folkerts et al,<sup>E2</sup> 10  $\mu$ g/mL ciprofloxacin was added to the culture medium as an antibiotic to prevent bacterial contamination. This concentration of ciprofloxacin was 20-fold lower than that of ciprofloxacin used for human MC degranulation assay. Cells were then cultured in Iscove modified Dulbecco medium (Thermo Fisher Scientific) with GlutaMAX-I (Thermo Fisher Scientific), 50  $\mu$ mol 2-mercaptoethanol, 0.5% (vol/vol) bovine serum albumin (Sigma-Aldrich), 1% (vol/vol) insulin-transferrin-selenium (Thermo Fisher Scientific), 10  $\mu$ g/mL ciprofloxacin, 50 ng/mL rhSCF, and 50 ng/mL rhIL-6 for 6 weeks. Cell purity was confirmed by analyzing the expression of c-Kit, Fc $\epsilon$ RI, and MRGPRX2 by flow cytometry.

### Flow cytometry

Before antibody staining, murine PCMCs were incubated for 10 minutes on ice with anti-mouse CD16/32 (Fc $\gamma$  III/II receptor) (70-0161; 1:1,000, Tonbo Biosciences, San Diego, Calif) to block Fc receptors. PCMCs were stained with the following antibodies: phycoerythrin (PE)-conjugated anti-mouse Fc $\epsilon$ RI (50-5898; 1:100, Tonbo Biosciences), biotinylated anti-mouse c-Kit (553353; 1:100, BD Biosciences), and allophycocyanin-conjugated streptavidin (554067; 1:500, BD Biosciences). To examine the effect of CS on cell viability, PCMCs were incubated for 3 hours with CS (25, 50, and 100  $\mu$ mol) or vehicle (0.1% DMSO) and stained with propidium iodide staining solution (BD Biosciences) according to the manufacturer's instructions. Human PBCMCs were stained with the following antibodies: allophycocyanin-conjugated anti-human Fc $\epsilon$ RI (334612; 1:100, BioLegend, San Diego, Calif), PE-conjugated anti-human c-Kit (313203; 1:100, BioLegend), and PE-conjugated anti-human MRGPRX2 (359004; 1:100, BioLegend). Flow cytometric analysis was performed with a BD FACSVerser device equipped with BD FACSuite software (BD Biosciences).

### Quantitative real-time PCR

Total RNA was extracted from PCMCs using the TRIzol Plus RNA Purification Kit (Thermo Fisher Scientific) according to the manufacturer's instructions. RNA purity and concentration were assessed by a NanoDrop device (ND-1000; Thermo Fisher Scientific). After treatment with RNase-free DNase I, RNA samples were reverse-transcribed with Oligo(dT)<sup>12-18</sup> primers and SuperScript III reverse transcriptase (Thermo Fisher Scientific) for amplification by PCR. Real-time PCR was performed on a CFX Connect Real-Time PCR Detection System (Bio-Rad, Hercules, Calif) using SYBR Green PCR Master Mix (Thermo Fisher Scientific). Target gene expression was normalized to that of *Hprt*. Melt curve analysis was performed to ensure the specificity of the amplification products. The following primers were used: *Hprt*, 5'-CTGGTGAAAAGGACCTCTCG-3' and 5'-TGAAGTACTCATTATAGTCAAGGGCA-3'; *Mrgprb2*, 5'-TACTTCTGCAGAGAGCCATGC-3' and 5'-GCTGCAGCTCTGAACAGTTTC-3'; *Fcer1a*, 5'-TGAATGTAACGCAA GATTGGCTG-3' and 5'-GCATCTGATGTCAAAGGATCCATG-3'; *Kit*, 5'-TGGCTTGATTAAGTCGGATGCT-3' and 5'-TTCAGTCCGACAT TAGGGCC-3'.

### MC degranulation assay

For the  $\beta$ -hexosaminidase release assay, supernatants (100  $\mu$ L) or cell lysates were incubated for 60 minutes at 37°C with 50  $\mu$ L of 1.3 mg/mL *p*-nitrophenyl-*N*-acetyl- $\beta$ -D-glucosaminide (Sigma-Aldrich) in 0.1 mol sodium citrate (pH 4.5). Cell lysates were prepared with 0.5% Triton X-100 in Tyrode buffer to analyze the total cellular content of  $\beta$ -hexosaminidase. The reaction was stopped by the addition of 150  $\mu$ L of 0.2 mol glycine-NaOH (pH 10.7), and the optical density at 405 nm was measured. The amount of  $\beta$ -hexosaminidase released was calculated as a percentage of the total content.

### Immunoblotting

PCMCs were lysed in 1 $\times$  cell lysis buffer (CST, Danvers, Mass) containing a cocktail of complete protease inhibitors (Roche, Basel, Switzerland). To assess the phosphorylation status, the PhosSTOP phosphatase inhibitor cocktail (Roche) was added to the cell lysis buffer. After centrifugation, supernatants were mixed with an equal volume of 2 $\times$  sample buffer (125 mmol Tris-HCl, 0.01% bromophenol blue, 4% SDS, 20% glycerol, and 200  $\mu$ mol dithiothreitol) and boiled for 5 minutes. Total protein concentration was measured by the DC Protein Assay Reagent (Bio-Rad). Samples were resolved via SDS-PAGE and transferred to a polyvinylidene fluoride membrane (Wako). Blots were probed with the following antibodies: rabbit anti-DOCK2 (09-454; 1:1000, Merck Millipore, Darmstadt, Germany), goat anti- $\beta$ -actin (sc-1616; 1:1000, Santa Cruz Biotechnology), rabbit anti-ERK1/2 (9102; 1:1000, CST), rabbit anti-p38 MAPK (9212; 1:1000, CST), rabbit anti-Akt (9272; 1:1000, C67E7, CST), goat anti-GSK3 $\beta$  (610202; 1:1000, BD Biosciences), and rabbit anti-PAK1 (ab223849; 1:1000, EPR20048, Abcam). Activation of ERK1/2, p38 MAPK, Akt, GSK3 $\beta$ , and PAK1 was assessed using phosphorylation-specific antibodies against Thr202/Tyr204 of ERK1/2 (4370; 1:1000, D13.14.4E, CST), Thr180/Tyr182 of p38 MAPK (9211; 1:1000, CST), Ser473 of Akt (4060; 1:1000, D9E, CST), Ser9 of GSK3 $\beta$  (9322; 1:1000, D3A4, CST), Ser144 of PAK1 and Ser141 of PAK2 (2606; 1:1000, CST), and Thr423 of PAK1 and Thr402 of PAK2 (2601; 1:1000, CST), respectively. The following horseradish peroxidase-conjugated secondary antibodies were used: mouse anti-rabbit IgG (sc-2357; 1:2,000, Santa Cruz Biotechnology), goat anti-mouse IgG (sc-2005; 1:2,000, Santa Cruz Biotechnology), and mouse anti-goat IgG (sc-2354; 1:2,000, Santa Cruz Biotechnology). Immunoreactive bands were quantified by ImageJ software (imagej.nih.gov/ij). After subtracting the background intensity, the ratio of phosphorylated protein to total protein was calculated.

Rac activation was assessed as described previously.<sup>E3,E4</sup> Before assay, cells were stimulated with 10  $\mu$ g/mL C48/80. Aliquots of cell extracts were kept as total lysate control samples, and the remaining extracts were incubated with agarose beads containing the GST-fusion Rac-binding domain of PAK1 (14-325; Merck Millipore) at 4°C for 60 minutes. The bound proteins and total cell lysates were resolved by SDS-PAGE. The blots

were probed with mouse anti-Rac1 (05-389; 1:2,000, 23A8, Merck Millipore) and mouse anti-Rac2 (WH0005880M1; 1:1000, 3B10-2D9, Sigma-Aldrich) antibodies. The ratio of GTP-bound Rac1/2 to total Rac1/2 was calculated by ImageJ software.

### **Toluidine blue staining**

Murine ear and back skin were collected and fixed with 4% paraformaldehyde (Wako) for 18 hours at 4°C. The dermis was washed with PBS and embedded in OCT compound (Sakura Finetek, Tokyo, Japan). After be-

ing frozen at  $-80^{\circ}\text{C}$ , cryostat sections were prepared at a thickness of 6  $\mu\text{m}$  and stained with 0.05% toluidine blue solution (pH 4.1; Wako) for 24 hours at room temperature. For PCMCs, samples were fixed with 4% paraformaldehyde for 1 hour at room temperature and mounted on glass slides with Smear Gell reagent (GenoStaff, Tokyo, Japan) according to the manufacturer's instructions. Then samples were stained with 0.05% toluidine blue solution for 24 hours at room temperature. Samples were dehydrated with 99.5% ethanol (Wako), mounted with coverslips, and examined by light microscopy. The number of skin MCs stained with toluidine blue metachromatically in the dermis was counted manually.

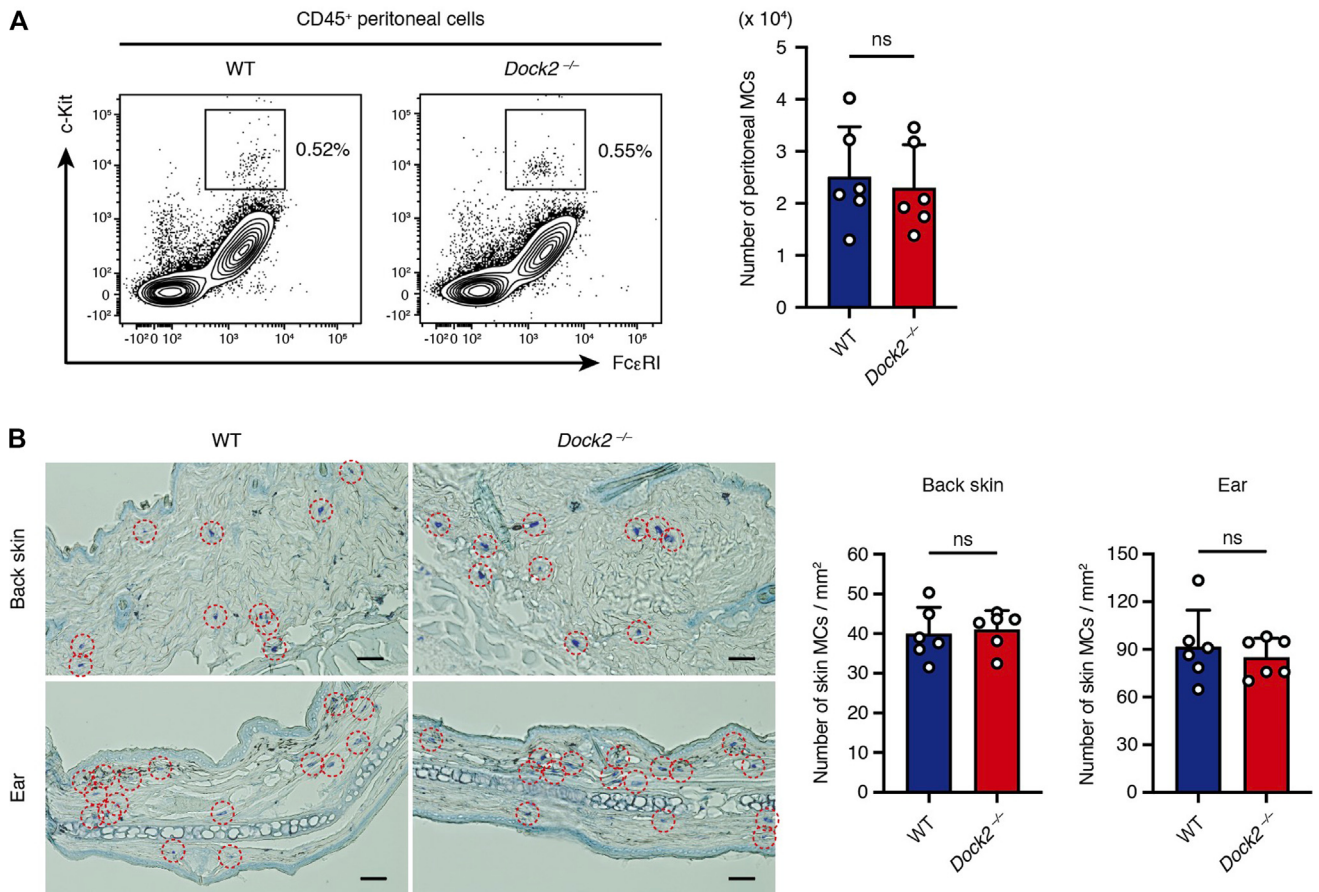


**FIG E1.** Comparison of MC numbers between WT and *Dock2*<sup>-/-</sup> mice. **A**, Flow cytometric analysis for MCs in peritoneal cavity from WT and *Dock2*<sup>-/-</sup> mice (left). Numbers indicate percentage of FcεRI<sup>+</sup>c-Kit<sup>+</sup> MCs in CD45<sup>+</sup> peritoneal cells. Absolute numbers of peritoneal MCs are shown at right (n = 6; 2-tailed unpaired Student *t* test). **B**, Representative images of MCs in back skin and ear collected from WT and *Dock2*<sup>-/-</sup> mice. Samples were stained with toluidine blue. Skin MCs are indicated by red dotted circles. Bar = 50 μm. Numbers of skin MCs per 1 mm<sup>2</sup> are shown at right (n = 6; 2-tailed unpaired Student *t* test). Data were collected from 2 (*A* and *B*) independent experiments and are shown as means ± SDs. NS, Not significant.

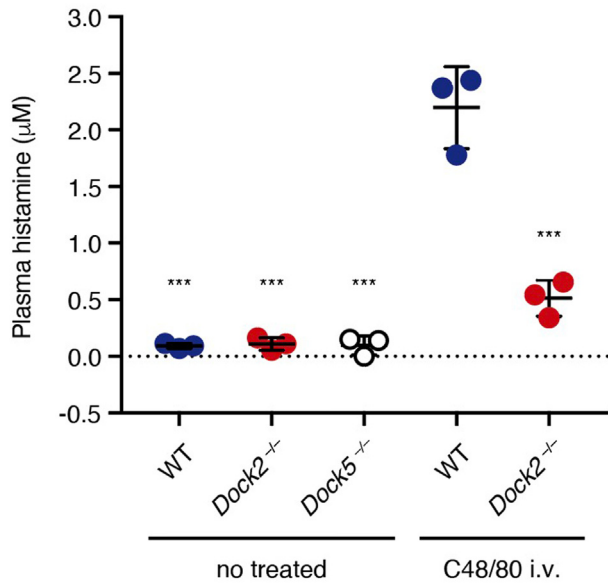


**FIG E2.** Plasma histamine concentrations in WT, *Dock2*<sup>-/-</sup>, and *Dock5*<sup>-/-</sup> mice before or 30 minutes after stimulation with 1.5 mg/kg C48/80 (n = 3; 1-way ANOVA with Dunnett multiple comparison test). Data were collected from 1 experiment and are shown as means ± SDs. \*\*\**P* < .001.

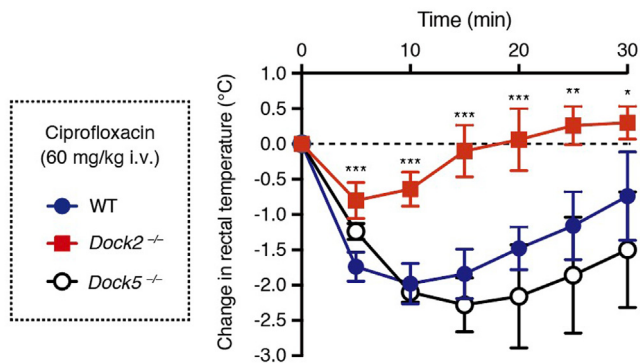


**FIG E3.** DOCK2 deficiency renders mice resistant to ciprofloxacin-induced systemic anaphylaxis. Change of rectal temperature in WT, *Dock2*<sup>-/-</sup>, and *Dock5*<sup>-/-</sup> mice challenged with ciprofloxacin (n = 5; 2-way repeated-measures ANOVA with Dunnett multiple comparisons test, versus WT group). Mice were injected intravenously (tail vein) with 100  $\mu$ L ciprofloxacin (60 mg/kg). Data were collected from 2 independent experiments and are shown as means  $\pm$  SDs. \**P* < .05; \*\**P* < .01; \*\*\**P* < .001.

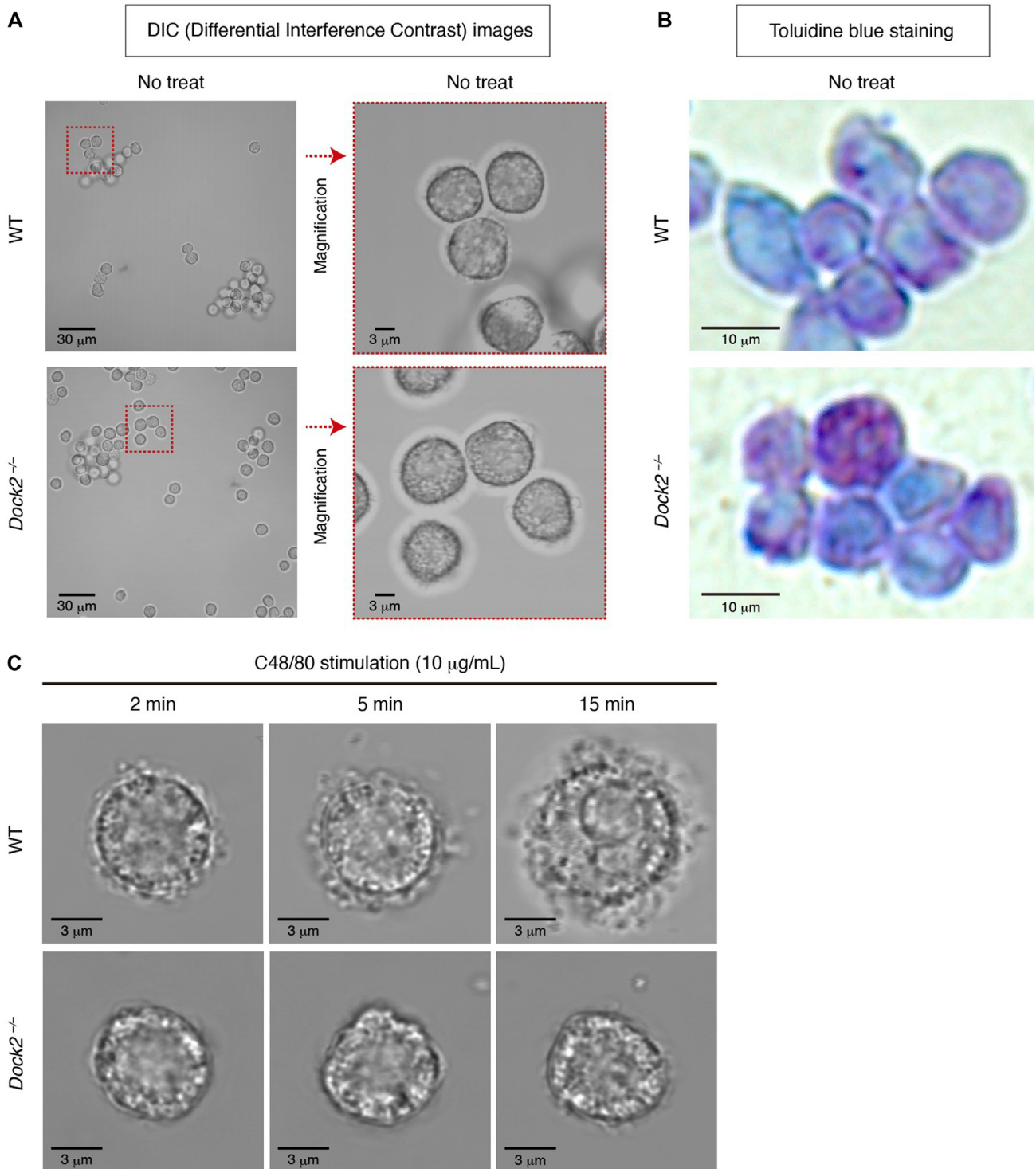


**FIG 4.** Morphology of PCMCs from WT and *Dock2*<sup>-/-</sup> mice, before and after C48/80 stimulation. **A**, Representative images of differential interference contrast (DIC) for nontreated WT and *Dock2*<sup>-/-</sup> PCMCs. Bar = 30  $\mu\text{m}$  (left) and 3  $\mu\text{m}$  (right). **B**, Representative images of toluidine blue staining for nontreated WT and *Dock2*<sup>-/-</sup> PCMCs. Bar = 10  $\mu\text{m}$ . **C**, Representative DIC images of C48/80-treated WT and *Dock2*<sup>-/-</sup> PCMCs, acquired with DIC. Bar = 3  $\mu\text{m}$ . Data were collected from 2 (A-C) independent experiments.



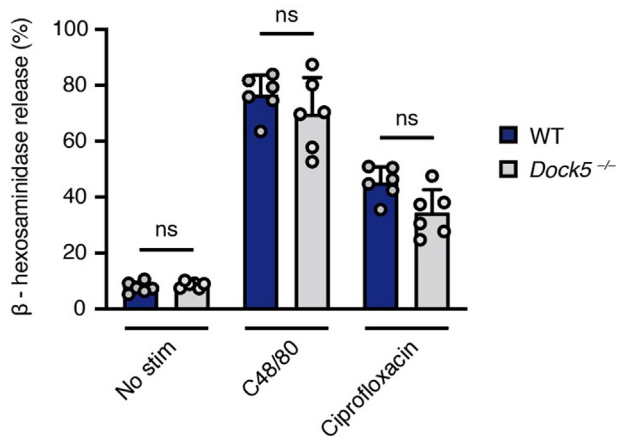


**FIG E5.** DOCK5 deficiency does not affect MRGPRB2-mediated MC degranulation. MRGPRB2-mediated degranulation of WT and *Dock5*<sup>-/-</sup> PCMCs was measured by β-hexosaminidase release assay after stimulation by C48/80 or ciprofloxacin (n = 6; 2-tailed unpaired Student *t* test). Data were collected from 2 independent experiments and are shown as means ± SDs. NS, Not significant.

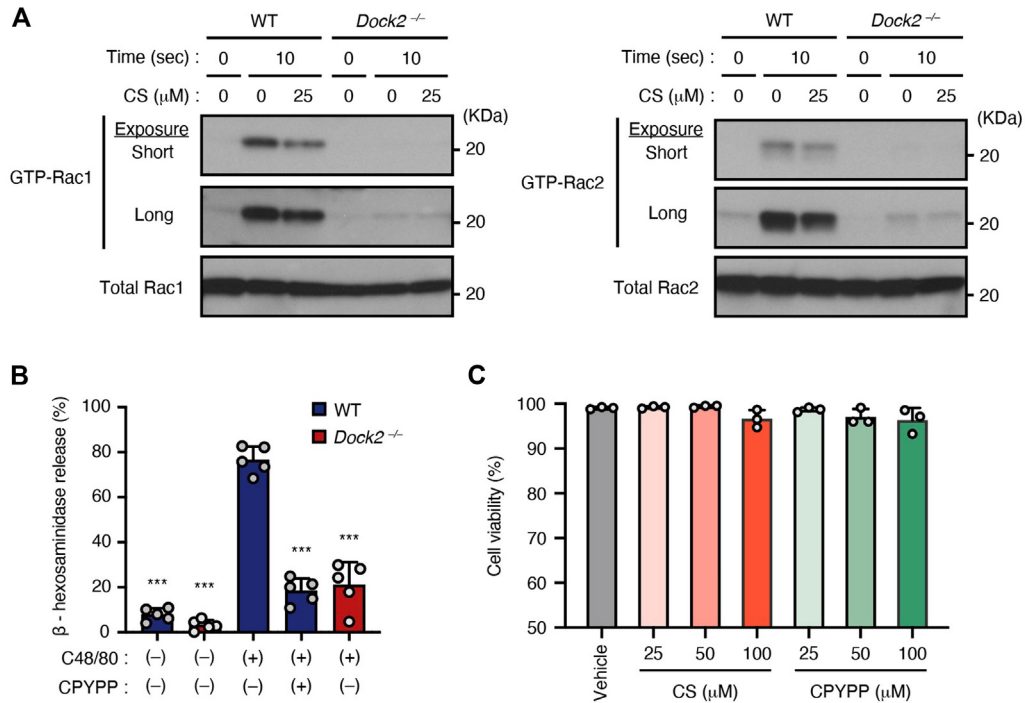


**FIG E6.** Effects of CS or CPYPP on MRGPRB2-mediated Rac activation and  $\beta$ -hexosaminidase release in WT and *Dock2*<sup>-/-</sup> PCMCs. **A**, Representative immunoblots showing C48/80-induced Rac activation in WT and *Dock2*<sup>-/-</sup> PCMCs in presence or absence of CS (25  $\mu$ M). **B**,  $\beta$ -Hexosaminidase release by WT and *Dock2*<sup>-/-</sup> PCMCs stimulated with C48/80 in presence or absence of CPYPP (50  $\mu$ M; n = 5; 1-way ANOVA with Dunnett multiple comparisons test). **C**, Viability of PCMCs was analyzed by flow cytometry after 3 hours of incubation with indicated concentrations of CS or CPYPP (n = 3). Data were collected from 2 (A), 5 (B), and 3 (C) independent experiments and are shown as means  $\pm$  SDs. \*\*\**P* < .001.

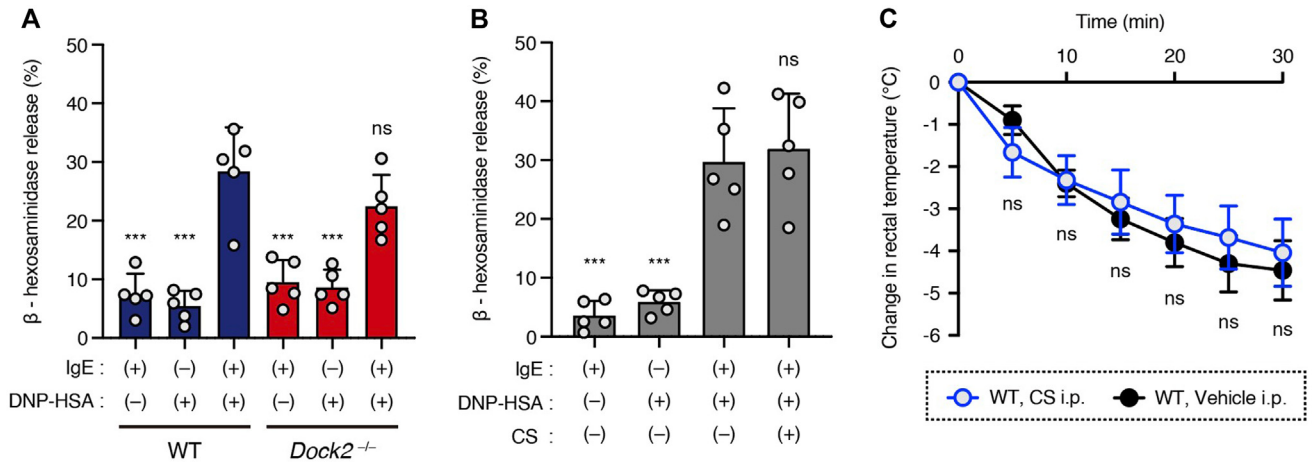


**FIG E7.** DOCK2 is not required for IgE-induced MC degranulation and systemic anaphylaxis. **A**, IgE-induced  $\beta$ -hexosaminidase release occurs normally even in the absence of DOCK2 ( $n = 5$ ; 1-way ANOVA with Dunnett multiple comparisons test). **B**, Treatment of WT-PCMCs with CS (25  $\mu$ mol) for 3 hours does not affect IgE-induced  $\beta$ -hexosaminidase release ( $n = 5$ ; 1-way ANOVA with Dunnett multiple comparisons test). **C**, After intraperitoneal administration of CS or vehicle, WT mice were challenged with IgE and DNP-HSA, and rectal temperature was monitored ( $n = 5$ , 2-way repeated-measures ANOVA with Bonferroni multiple comparison test). Data were collected from 5 (**A** and **B**) and 2 (**C**) independent experiments and are presented as means  $\pm$  SDs. \*\*\* $P < .001$ . NS, Not significant.